Eur Spine J (2012) 21:1950–1956
DOI 10.1007/s00586-012-2356-2

ORIGINAL ARTICLE

Sagittal balance correction of idiopathic scoliosis using the in situ contouring technique

Yann Philippe Charles · Julia Bouchaïb · Axel Walter · Sébastien Schuller · Erik André Sauleau · Jean-Paul Steib

Received: 29 December 2011 / Revised: 15 April 2012 / Accepted: 25 April 2012 / Published online: 8 June 2012

Abstract
Purpose Idiopathic scoliosis can lead to sagittal imbalance. The relationship between thoracic hyper- and hypokyphotic segments, vertebral rotation and coronal curve was determined. The effect of segmental sagittal correction by in situ contouring was analyzed.
Methods Pre- and post-operative radiographs of 54 scoliosis patients (Lenke 1 and 3) were analyzed at 8 years follow-up. Cobb angles and vertebral rotation were determined. Sagittal measurements were: kyphosis T4–T12, T4–T8 and T9–T12, lordosis L1–S1, T12–L2 and L3–S1, pelvic incidence, pelvic tilt, sacral slope, T1 and T9 tilt.
Results Thoracic and lumbar curves were significantly reduced ($p = 0.0001$). Spino-pelvic parameters, T1 and T9 tilt were not modified. The global T4–T12 kyphosis decreased by 2.1° on average ($p = 0.066$). Segmental analysis evidenced a significant decrease of T4–T8 hyperkyphosis by 6.6° ($p = 0.0001$) and an increase of segmental hypokyphosis T9–T12 by 5.0° ($p = 0.0001$). Maximal vertebral rotation was located at T7, T8 or T9 and correlated ($r = 0.422$) with the cranial level of the hypokyphotic zone ($p = 0.003$). This vertebra or its adjacent levels corresponded to the coronal apex in 79.6 % of thoracic curves.
Conclusions Lenke 1 and 3 curves can show normal global kyphosis, divided in cranial hyperkyphosis and caudal hypokyphosis. The cranial end of hypokyphosis corresponds to maximal rotation. These vertebrae have most migrated anteriorly and laterally. The sagittal apex between segmental hypo- and hyper-kyphosis corresponds to the coronal thoracic apex. A segmental sagittal imbalance correction is achieved by in situ contouring. The concept of segmental imbalance is useful when determining the levels on which surgical detorsion may be focused.

Keywords Idiopathic scoliosis · Sagittal balance · Thoracic kyphosis · Vertebral rotation · Posterior instrumentation · In situ contouring

Introduction

Idiopathic scoliosis represents a three-dimensional (3D) spinal deformity involving coronal, sagittal and transversal planes. Top views of the spine were used to understand the phenomenon of vertebral migration during scoliosis progression [1, 2]. In thoracic curves, vertebral rotation leads to an anterior and lateral vertebral displacement. In lumbar curves, vertebral migration follows a posterior and lateral direction.

A variety of instrumentations exist, aimed to obtain a balanced spine. The Cotrel–Dubousset technique first attempted to correct kyphosis by rod derotation [3]. Modern approaches using segmental pedicle screw fixation act by direct vertebral derotation [4]. Simultaneous two-rod translation [5] or vertebral coplanar alignment [6] enables to restore kyphosis in thoracic curves. In situ contouring uses a rod that follows the shape of the scoliotic spine, which is then bent to correct the 3D deformity sequentially [7].

Y. P. Charles (✉) · J. Bouchaïb · A. Walter · S. Schuller · J.-P. Steib
Service de Chirurgie du Rachis, Hôpitaux Universitaires de Strasbourg, 1, Place de l'Hôpital, B.P. 426, 67091 Strasbourg Cedex, France
e-mail: yann.philippe.charles@chru-strasbourg.fr

E. A. Sauleau
Département de Santé Publique, Hôpitaux Universitaires de Strasbourg, Strasbourg Cedex, France

Although these methods seem to facilitate reduction, thoracic kyphosis correction remains a concern and preoperative planning is crucial to achieve an adequate sagittal balance.

The Lenke classification [8] offers a comprehensive radiographic evaluation since coronal curves and their flexibilities, lumbar modifiers and the sagittal profile are considered. However, the amount of vertebral rotation and the selection of instrumented vertebrae which would allow the best detorsion may not be predicted. Computer simulation has been advocated to optimize instrumentation strategies [9]. Patient-specific finite element analyses may improve the prediction of correction mechanisms [10]. Although these aids of 3D assessment are interesting, their use remains difficult clinically. It would be valuable to find simple markers describing the relationship between rotation, sagittal imbalance and coronal deformity on radiographs.

The purpose of this study was to determine the effect of in situ contouring on global and segmental sagittal thoracolumbar alignment. The relationship between hyper- and hypokyphotic thoracic segments, vertebral rotation and coronal curve pattern was retrospectively analyzed, seeking for radiographic markers that may facilitate surgical planning to improve sagittal balance.

Materials and methods

Institutional review board approval was obtained. Medical records of 157 consecutive patients followed for adolescent idiopathic scoliosis and operated as young adults between 1994 and 2007 were reviewed. The preoperative radiographs were screened for a particular sagittal pattern representing the inclusion criteria: cranial hyperkyphosis and caudal hypokyphosis of the thoracic spine (Fig. 1). Global flat backs, thoracic lordosis or hyperkyphosis were excluded. The sagittal full spine radiographs of 54 patients (34.4 %) showed the required mixed pattern in the thoracic spine. The cohort was composed of 6 males and 48 females. The average age at surgery was 21.4 (19–29) years and the follow-up was 8.0 (3.5–15.7) years. Curves were classified as 27 Lenke 1 and 27 Lenke 3. Sagittal thoracic modifiers −, N, or + were present in both subgroups.

Surgery was indicated in progressive imbalance and curves >45°. A single posterior instrumentation was performed in 28 patients with >50 % reducible curves on side bending radiographs. A thoracoscopic release was indicated in 26 patients for structural curves >70°. A posterior facet release was performed prior to instrumentation. In situ contouring was used for deformity correction: the rod first took the shape of the scoliotic spine, which then followed the shape of the working rod that was progressively bent inside the patient. It was placed on the concave side of the thoracic curve and the convex side of the lumbar curve. Hybrid constructs were used with pedicle hooks at thoracic levels and monoaxial pedicle screws in the lower thoracic and lumbar spine. The rod was locked onto a pediculo-transverse or pediculo-laminar claw at the cranial extremity. All other rod–hook and rod–screw connections remained unlocked at 90°, thus allowing free implant rotation around the rod, while bending the rod and transmitting correction maneuvers to the spine. Correction was achieved successively at different levels by alternating medialisation and anterior pressure of lumbar vertebrae, pushing hypolordotic zones of the lumbar spine anteriorly, while progressive derotation was applied (Fig. 2). The thoracic deformity was corrected by segmental medialisation, posterior traction and derotation, pulling hypokyphotic zones of the thoracic spine posteriorly (Fig. 3). These maneuvers allowed a spinal detorsion following the reverse way of scoliosis formation.

Fig. 1 Right thoracic curve in the coronal plane with cranial hyperkyphosis (*white arrow*) and caudal hypokyphosis (*black arrow*) in the sagittal plane

Preoperative and last postoperative radiographs were digitized using an optical scanner (VIDAR TWAIN 32, Vidar systems Inc, Herndon, Virginia). Measurements were performed with Spineview software (Surgiview, Paris, France) [11]. Cobb angles were measured [12] and apical vertebrae were determined on posteroanterior full spine standing radiographs. Sagittal balance was assessed on lateral full spine radiographs including femoral heads. Thoracic kyphosis was measured between the superior T4 endplate and the inferior T12 endplate. This measurement was divided into a cranial kyphosis between T4 and T8,

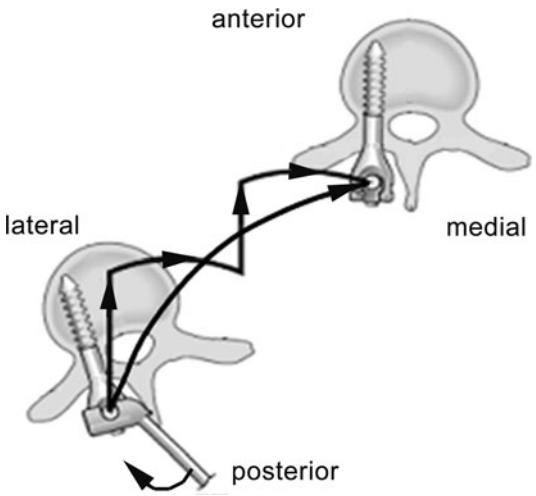

Fig. 2 Correction pathway (*continuous curved line*) using in situ contouring at lumbar levels, pushing vertebrae successively forward (increasing lordosis) and medial (correction of coronal curve) while derotating on convex sided screws with a lever arm

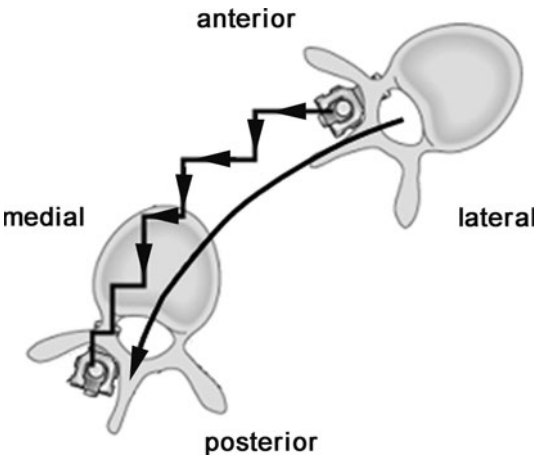

Fig. 3 Correction pathway (*continuous curved line*) using in situ contouring at thoracic levels, pulling vertebrae successively backward (increasing kyphosis) and medial (correction of coronal curve) using pedicle hooks on the concave side of the curve

and a caudal kyphosis between T9 and T12. Lumbar lordosis was determined between the superior L1 endplate and the S1 endplate. The cranial lordosis was measured between T12 and L2 and the caudal the caudal lordosis between L3 and S1. Global sagittal balance was assessed using the T1 and T9 tilt: angles between the vertical axis passing through the middle of both femoral heads' centers and two axes passing through the center of T1 and T9 vertebral bodies, respectively. Sagittal spino-pelvic balance was determined by pelvic incidence, pelvic tilt and sacral slope [13].

Vertebral rotation was assessed preoperatively to define the level of the most rotated thoracic vertebra. The most rotated lumbar vertebra was documented only in Lenke three curves. Vertebral rotation was measured on postero-anterior standing radiographs according to Perdriolle [14] and on CT reconstructions of each vertebra from T1 to L5, passing through the plane parallel to the cranial endplate at the pedicles' level. The angle was built between the longitudinal vertebral body axis passing through the middle of the posterior wall and the vertical axis of the CT image [15]. Postoperatively, vertebral rotation was not evaluated because the instrumentation would prevent proper radiographic evaluation and control CT was not performed.

The number of vertebrae included in a caudal thoracic hypokyphotic zone (HKZ), including the thoracolumbar junction, was counted on preoperative lateral radiographs. The most cranial and caudal vertebrae of this HKZ were noted. The cranial level was compared to the level of the thoracic apical vertebra on posteroanterior radiographs. A comparison was made between the caudal level of the HKZ and the lumbar apical vertebra in Lenke 3 curves. The level of most rotated thoracic vertebra was compared to the cranial level, and the maximally rotated vertebra of lumbar curves to the caudal level of the HKZ.

Statistical analysis

Statistical evaluation was performed with SPSS 16.0 (SPSS Inc, Chicago, IL). Student's *t* test was used for the pre- and post-operative comparison of normally distributed radiographic measurements. The Wilcoxon test was used for the analysis of T4–T8 kyphosis, T9–T12 kyphosis, T12–L2 lordosis and L3–S1 lordosis. The correlation coefficient of Spearman was used to analyze the relationships between the most cranial vertebra of the HKZ, vertebral rotation and the apical thoracic vertebra. The same applied for the relationship between the caudal level of the HKZ, vertebral rotation and the apical lumbar vertebra. The correlation was considered as excellent if the Spearman correlation coefficient was >0.80, good 0.61–0.80, middle 0.41–0.60, and poor ≤0.40. The significance level was set at 0.05.

Results

Global coronal and sagittal balance

Coronal thoracic and lumbar curves were significantly reduced (Table 1). There was no modification of sagittal T1 and T9 tilt. The same applied to dynamic sagittal spino-pelvic parameters pelvic tilt and sacral slope. The intrinsic anatomical spino-pelvic configuration of pelvic incidence remained stable. Thoracic kyphosis T4–T12 decreased by 2.1° and lumbar lordosis L1–S1 decreased by 2.2°.

Table 1 Comparison of pre- and post-operative Cobb angles and global sagittal radiographic parameters in degrees

	Preoperative average ± SD	Range	Postoperative average ± SD	Range	*t* test
Thoracic Cobb	59.8 ± 16.1	36–104	21.2 ± 13.5	0–70	$p = 0.0001$
Lumbar Cobb[a]	50.4 ± 15.9	28–88	20.2 ± 14.8	0–53	$p = 0.0001$
T4–T12 kyphosis	28.2 ± 13.3	7–58	26.1 ± 10.8	9–61	$p = 0.066$
L1–S1 lordosis	49.9 ± 12.3	16–72	47.7 ± 10.3	22–69	$p = 0.154$
T1 tilt	3.2 ± 3.0	0–16	3.6 ± 2.4	0–11	$p = 0.419$
T9 tilt	6.0 ± 4.3	0–17	5.8 ± 4.0	0–18	$p = 0.808$
Pelvic incidence	49.3 ± 10.7	23–74	49.5 ± 11.1	20–75	$p = 0.708$
Pelvic tilt	8.7 ± 5.9	0–24	10.7 ± 6.6	0–30	$p = 0.070$
Sacral slope	40.4 ± 7.9	21–62	38.6 ± 8.9	16–56	$p = 0.740$

[a] Measured for double major curves type Lenke 3 only

Segmental correction of thoracic kyphosis and lumbar lordosis

The cranial hyperkyphotic segment T4–T8 decreased by 6.6° and the caudal hypokyphotic segment T9–T12 increased by 5.0°. T12–L2 lordosis increased by 3.7° and L3–S1 lordosis decreased by 3.2° (Table 2).

Relationship between vertebral rotation, apical vertebrae and sagittal imbalance

The maximally rotated vertebra was located between T6 and T10 for thoracic curves (Lenke 1 and 3) and between L1 and L3 for lumbar curves (Lenke 3). The average rotation of the maximally rotated thoracic vertebra was 22.7° ± 7.9° (10°–45°) on radiographs and 18.9° ± 7.1° (5°–36°) on CT. The average rotation of the maximally rotated lumbar vertebra was 25.8° ± 7.7° (15°–45°) on radiographs and 22.0° ± 8.3° (10°–36°) on CT.

In the coronal plane, the apical vertebra was located between T7 and T10 for thoracic curves (Lenke 1 and 3) and between L1 and L3 for lumbar curves (Lenke 3). In the sagittal plane, the HKZ, appearing as an extension of the physiological T12–L1 rectitude, was observed between T7 and L2. The number of vertebrae included in the HKZ was 6 or 7. The most cranial vertebra of the HKZ corresponded to T7 in 6 patients, T8 in 26 patients and T9 in 22 patients. The caudal vertebra of the HKZ was usually L1 in Lenke 1 and L2 in Lenke 3 curves.

The correlation between cranial level of HKZ, most rotated and apical thoracic vertebra, as well as the correlation between caudal level of HKZ, most rotated and lumbar apical vertebra are demonstrated in Table 3. It appeared that only the cranial level of HKZ and the level of most rotated thoracic vertebra were significantly ($p = 0.003$) correlated. The cranial vertebra of HKZ or its adjacent level in the sagittal plane corresponded to the most rotated vertebra in 46/54 patients (85.2 %) in the transversal plane, and to the apical vertebra in 43/54 patients (79.6 %) in the frontal plane. The relationship between vertebral rotation, cranial vertebra of HKZ and apical vertebra is shown in Fig. 4. This level represents the turning point of maximal vertebral rotation that divides global thoracic kyphosis in a caudal hypokyphosis and an adjacent cranial hyperkyphosis. It also represents the level of the thoracic vertebra that has most migrated anteriorly and laterally in space, corresponding to the apex of the deformity.

Discussion

Coronal curve reduction is obtained by several posterior instrumentation techniques including in situ contouring [4–7]. Sagittal alignment influences the long-term outcome of instrumented and mobile segments [5]. This implies a complete understanding of 3D deformity to establish the correction strategy [16]. Only a few studies have analyzed

Table 2 Comparison of pre- and postoperative segmental kyphosis and lordosis in degrees

	Preoperative average ± SD	Range	Postoperative average ± SD	Range	Wilcoxon test
T4–T8 kyphosis	24.0 ± 11.4	5–49	17.4 ± 9.6	5–44	$p = 0.0001$
T9–T12 kyphosis	3.6 ± 2.9	0–12	8.6 ± 4.1	0–22	$p = 0.0001$
T12–L2 lordosis	6.7 ± 4.2	0–17	10.4 ± 4.7	2–24	$p = 0.027$
L3–S1 lordosis	42.1 ± 11.7	12–63	38.9 ± 9.9	17–60	$p = 0.463$

Table 3 Correlation between cranial vertebra of sagittal hypokyphotic zone (HKZ), most rotated thoracic vertebra and apical thoracic vertebra in Lenke type 1 and 3 curves

	Spearman correlation	Significance
Cranial level–rot max thoracic	$r = 0.422$	$p = 0.003$
Cranial level–apical thoracic	$r = 0.133$	$p = 0.357$
Caudal level–rot max lumbar	$r = 0.290$	$p = 0.145$
Caudal level–apical lumbar	$r = 0.136$	$p = 0.393$

Correlation between caudal vertebra of the HKZ, most rotated lumbar vertebra and apical lumbar vertebra in Lenke type 3 curves

the sagittal thoracic profile in detail. Most authors do not differentiate between normal, hypo- or hyperkyphosis, and patients with both types of sagittal deformity at different levels.

The Cotrel–Dubousset derotation technique led to an average thoracic kyphosis increase of 8.7° according to Bjerkreim et al. [17]. Sucato et al. [18] reported that hook constructs increased kyphosis by 1.9° versus 0.4° with hybrid hook–screw instrumentations. Lee et al. [4] showed a kyphosis increase of 7° with direct vertebral rotation versus 5° with entire rod derotation using pedicle screws. Clement et al. [5] reported a 5.8° kyphosis increase with cantilever reduction versus 15.8° with simultaneous two-rod translation. Schmidt et al. [19] demonstrated a kyphosis increase of 13.2° with anterior dual rod instrumentation in thoracic lordoscoliosis, compared to 5.3° with posterior pedicle screw instrumentation. A kyphosis decrease was observed with any kind of instrumentation by Lowenstein et al. [20] and Kim et al. [21] who compared all pedicle screws versus hybrid or hook constructs. The modification of sagittal alignment may depend on the technique, but the amount and pattern of initial deformity remains crucial. Our patients presented a mixture between a caudal flat back (HKZ) and an adjacent cranial hyperkyphosis, which explains why the global kyphosis decrease of 2.1° was not significant.

Kotwicki [22] pointed out that global kyphosis measurements were misleading because curves presenting the same coronal plane deformity could differ morphologically in the two other planes. He emphasized detailed kyphosis measurements between T5–T8 and T9–T12 to differentiate hyper- and hypokyphotic zones. The average kyphosis of 15.8° between T5 and T8 and 3.9° between T9 and T12 indicated a segmental imbalance related to the thoracic curve type, as confirmed by our results. In situ contouring achieved a harmonious sagittal thoracic balance: cranial hyperkyphosis T4–T8 decreased, caudal hypokyphosis T9–T12 (HKZ) increased, and lordosis increased between T12 and L2 (Fig. 5).

Katsuhiro et al. [23] demonstrated that a standard lateral radiograph would not properly image kyphosis. A 13° trunk rotation would show the real, usually underestimated, T8–T11 hypokyphosis. This phenomenon is related to the torsion of the spine: the maximally rotated thoracic vertebrae move anterior and laterally, which increases the curve in the coronal plane and decreases segmental kyphosis in the sagittal plane. Sangole et al. [24] demonstrated the existence of different subgroups within Lenke 1 curves, suggesting that thoracic scoliosis could be normo- or hypokyphotic (Fig. 6). Stokes et al. [25] used top views to demonstrate that sagittal apex, coronal apex and vertebral rotation were closely related. Rotation of the plane of maximal curvature was very sensitive to sagittal plane

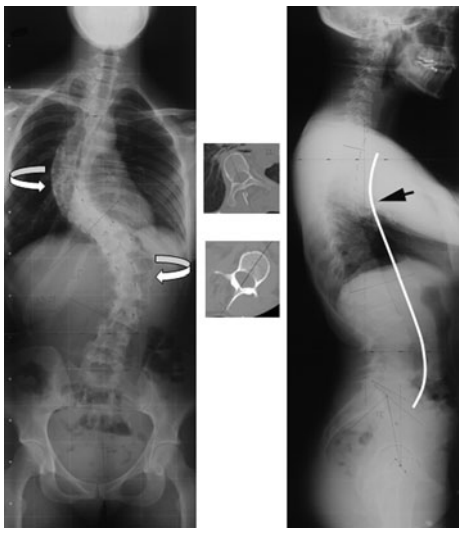

Fig. 4 Relationship between maximally rotated thoracic and lumbar vertebrae, apical vertebrae and sagittal hyphokyphotic zone. The cranial extremity of this zone (*black arrow*) corresponds to the turning point of the thoracic curve and separates caudal hypokyphosis and cranial hyperkyphosis

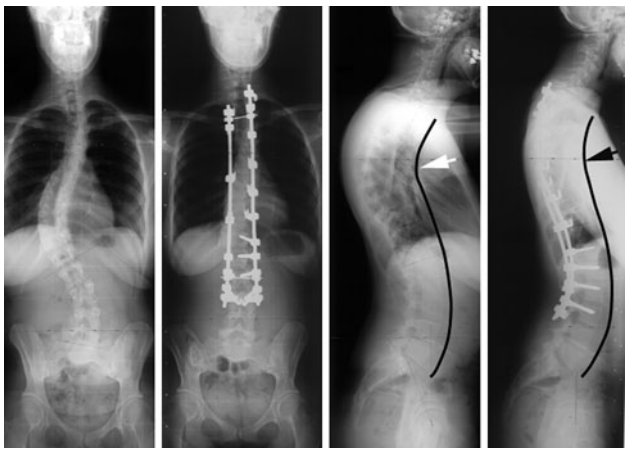

Fig. 5 Coronal curve correction and thoracic sagittal imbalance with cranial hyperkyphosis and caudal hypokyphosis before (*white arrow*) and after (*black arrow*) in situ contouring

Fig. 6 Comparison of two types of thoracic scoliosis with different sagittal plane deformities: global hypokyphosis (flat back) on the *left* and globally normal kyphosis (cranial hyperkyphosis and caudal hypokyphosis) on the *right*

changes, especially when the sagittal thoracic curvature was small. Our observations confirm their theory: a short thoracic kyphosis (the turning point between the HKZ and the cranial hyperkyphosis) corresponds to maximal rotation (Fig. 4). This has implications for posterior instrumentation techniques, since procedures associated with apical vertebral derotation may exposed it to the risk of further decrease in thoracic kyphosis if 3D relationships are not properly analyzed [23].

Perdriolle and Vidal [14] emphasized vertebral rotation which increases as thoracic curves become progressive. Kotwicki [22] measured maximal rotation around T9 (10°–24°) in thoracic curves with caudal hypokyphosis and cranial hyperkyphosis. Rotation decreased in adjacent vertebrae and was almost neutral around L1. Our results were concordant with these findings. The maximally rotated thoracic vertebra located between T6 and T10 correlated with the cranial HKZ levels T8–T9. Surgical correction by derotation should therefore focus on the sagittal apex dividing hypo- and hyperkyphotic zones, corresponding to the zone of maximal thoracic rotation. Direct apical vertebral rotation using pedicle screws led to a 7.1° decrease versus a 1.6° decrease using simple rod derotation [4]. The detorsion effect of in situ contouring has not been measured on control CT in our study, but had been previously evaluated, showing that maximal thoracic rotation decreased by 12° and a maximal lumbar rotation by 8° [7].

The sagittal deformity remains critical since a flat back might lead to progressive decompensation and anterior imbalance [26]. Pelvic incidence has a fundamental influence on spinal balance. Upasani et al. [27] showed that patients with Lenke 1 curves had an increased pelvic incidence and sacral slope, and a decreased thoracic kyphosis. This configuration describes a sagittal imbalance of patients that would physiologically have a large lumbar lordosis and thoracic kyphosis [26]. Because of vertebral rotation and anterior migration of the caudal thoracic spine, hypokyphosis may lead to a flat back. Lenke 1 curves can be hypokyphotic in some patients and normokyphotic in other patients when considering only the global kyphosis (Fig. 6). Mac-Thiong et al. [13] demonstrated that thoracic kyphosis was lower for thoracic than lumbar curves. Thoracic kyphosis depends on 3D deformity and is related to the coronal curve. Lumbar lordosis is highly influenced by the spino-pelvic configuration. There is a strong relationship between lumbar lordosis and the sagittal pelvic orientation [26]. Pelvic incidence, pelvic tilt and sacral slope ranged within physiological values in our study, which indicates that the sagittal deformity in Lenke 1 and 3 curves is probably less related to the spino-pelvic configuration, rather than the thoracic deformity itself.

Conclusion

Lenke 1 and 3 curves can present a normal kyphosis, divided into cranial hyperkyphosis and caudal hypokyphosis (HKZ). Vertebral rotation is maximal at the cranial levels of the HKZ. These vertebrae are located around the sagittal and coronal apex. In situ contouring improved sagittal balance by segmental detorsion and restoration of segmental kyphosis and lordosis. The concept of HKZ and segmental imbalance represents a useful indicator when determining the levels of main spinal torsion preoperatively.

Conflict of interest None.

References

1. Graf H, Hecquet J, Dubousset J (1983) Approche tridimensionnelle des déformations rachidiennes. Application à l'étude des scolioses infantiles. Rev Chir Orthop Reparatrice Appar Mot 69:407–416
2. Kohashi Y, Oga M, Sugioka Y (1996) A new method using top views of the spine to predict the progression of curves in idiopathic scoliosis during growth. Spine 21:212–217
3. Cotrel Y, Dubousset J, Guillaumat M (1988) New universal instrumentation in spinal surgery. Clin Orthop Relat Res 227:10–23
4. Lee SM, Suk SI, Chung ER (2004) Direct vertebral rotation: a new technique of three-dimensional deformity correction with segmental pedicle screw fixation in adolescent idiopathic scoliosis. Spine 29:343–349
5. Clement JL, Chau E, Kimkpe C, Vallade MJ (2008) Restoration of thoracic kyphosis by posterior instrumentation in adolescent idiopathic scoliosis. Comparative radiographic analysis of two methods of reduction. Spine 33:1579–1587

6. Vallespir GP, Flores JB, Trigueros IS, Sierra EH, Fernández PD, Olaverri JC, Alonso MG, Galea RR, Francisco AP, Rodríguez de Paz B, Carbonell PG, Thomas JV, López JL, Paulino JI, Pitarque CB, García OR (2008) Vertebral coplanar alignment: a standardized technique for three dimensional correction in scoliosis surgery: technical description and preliminary results in Lenke type 1 curves. Spine 33:1588–1597
7. Steib JP, Dumas R, Mitton D, Skalli W (2004) Surgical correction of scoliosis by in situ contouring: a detorsion analysis. Spine 29:193–199
8. Lenke KH, Betz RR, Harms J, Bridwell KH, Clements DH, Lowe TG, Blanke K (2001) Adolescent idiopathic scoliosis: a new classification to determine extent of spinal arthrodesis. J Bone Joint Surg Am 83:1169–1181
9. Majdouline Y, Aubin CE, Sangole A, Labelle H (2009) Computer simulation for the optimization of instrumentation strategies in adolescent idiopathic scoliosis. Med Biol Eng Comput 47:1143–1154
10. Lafon Y, Steib JP, Skalli W (2010) Intraoperative three dimensional correction during in situ contouring surgery by using a numerical model. Spine 35:453–459
11. Vialle R, Ilharreborde B, Dauzac C, Guigui P (2006) Intra and inter-observer reliability of determining degree of pelvic incidence in high-grade spondylolisthesis using a computer assisted method. Eur Spine J 15:1449–1453
12. Cobb JR (1960) The problem of the primary curve. J Bone Joint Surg Am 42:1413–1425
13. Mac-Thiong JM, Labelle H, Charlebois M, Huot MP, de Guise JA (2003) Sagittal plane analysis of the spine and pelvis in adolescent idiopathic scoliosis according to the coronal curve type. Spine 28:1404–1409
14. Perdriolle R, Vidal J (1985) Thoracic idiopathic scoliosis curve evolution and progression. Spine 10:785–791
15. Ho EKW, Upadhyay SS, Chan FL, Hsu LC, Leong JC (1993) New methods of measuring vertebral rotation from computed tomographic scans. Spine 18:1173–1177
16. Bakaloudis G, Lolli F, Di Silvestre M, Greggi T, Astolfi S, Martikos K, Vommaro F, Barbanti-Brodano G, Cioni A, Giacomini S (2011) Thoracic pedicle subtraction osteotomy in the treatment of severe pediatric deformities. Eur Spine J 20(Suppl 1):S95–S104
17. Bjerkreim I, Steen H, Brox JI (2007) Idiopathic scoliosis treated with Cotrel-Dubousset instrumentation: evaluation 10 years after surgery. Spine 32:2103–2110
18. Sucato DJ, Agrawal S, O'Brien MF, Lowe TG, Richards SB, Lenke L (2008) Restoration of thoracic kyphosis after operative treatment of adolescent idiopathic scoliosis. A multicenter comparison of three surgical approaches. Spine 33:2630–2636
19. Schmidt C, Liljenqvist U, Lerner T, Schulte TL, Bullmann V (2011) Sagittal balance of thoracic lordoscoliosis: anterior dual rod instrumentation versus posterior pedicle screw fixation. Eur Spine J 20:1118–1126
20. Lowenstein JE, Matsumoto H, Vitale MG, Weidenbaum M, Gomez JA, Lee FY, Hyman JE, Roye DP Jr (2007) Coronal and sagittal plane correction in adolescent idiopathic scoliosis comparison between all pedicle screws versus hybrid thoracic hook lumbar screw constructs. Spine 32:448–452
21. Kim YJ, Lenke LG, Cho SK, Bridwell KH, Sides B, Blanke K (2004) Comparative analysis of pedicle screw versus hook instrumentation in posterior spinal fusion of adolescent idiopathic scoliosis. Spine 29:2040–2048
22. Kotwicki T (2002) Sagittal and transversal plane deformity in thoracic scoliosis. Stud Health Technol Inform 91:251–256
23. Katsuhiro H, Upasani VV, Pawelek JB, Aubin CE, Labelle H, Lenke LG, Jackson R, Newton PO (2009) Three-dimensional analysis of thoracic apical sagittal alignment in adolescent idiopathic scoliosis. Spine 34:792–797
24. Sangole AP, Aubin CE, Labelle H, Stokes IA, Lenke LG, Jackson R, Newton P (2009) Three-dimensional classification of thoracic scoliotic curves. Spine 34:91–99
25. Stokes IAF, Sangole AP, Aubin CE (2009) Classification of scoliosis deformity three-dimensional spinal shape by cluster analysis. Spine 34:584–590
26. Roussouly P, Nnadi C (2010) Sagittal plane deformity: an overview of interpretation and management. Eur Spine J 19:1824–1836
27. Upasani VV, Tis J, Pawelek J, Pawelek J, Marks M, Lonner B, Crawford A, Newton PO (2007) Analysis of sagittal alignment in thoracic and thoracolumbar curves in adolescent idiopathic scoliosis: how do these two curve types differ? Spine 32:1355–1359